

# RESIDUAL STRESSES IN THE JOINT OF THE COLLECTOR TO THE DN1200 NOZZLE OF THE PGV-1000 STEAM GENERATOR DUE TO LOCAL HEAT TREATMENT

**O.V. Makhnenko, O.F. Muzhychenko, I.I. Prudkiy, N.R. Basistyuk**

E.O. Paton Electric Welding Institute of the NASU  
11 Kazymyr Malevych Str., 03150, Kyiv, Ukraine

## ABSTRACT

When assessing the extension of the service life of WVER-1000 NPP power units, the welded joint of the collector to the DN1200 nozzle of the PGV-1000 steam generator is an object of increased attention due to its tendency to the formation of discontinuity defects. In order to obtain more detailed information regarding the loading of this welded joint, mathematical modeling of the kinetics of formation of residual stresses and plastic strains, as a result of local postweld heat treatment in the high-temperature tempering mode, was carried out using the finite element method. The complex geometry of the joint and the local arrangement of the heaters cause significant nonuniformity of heating during heat treatment, which can lead to negative consequences, namely, formation of high residual tensile stresses in the dangerous zones of the welded joint. It is proven that the axisymmetric 2D finite element model of the joint with the shortest length of the DN1200 nozzle provides sufficient conservatism of the results compared to the general 3D model.

**KEYWORDS:** PGV-1000 steam generator, welded joint No. 111, local heat treatment, residual stresses, plastic strains, mathematical modeling, creep

## INTRODUCTION

Over the past twenty years, during the operation of WVER-1000 power units at the Ukrainian NPP, material discontinuity defects have been repeatedly detected in the welded joint between the collector and the DN1200 nozzle of the PGV-1000 steam generators welded joint No.111, which is part of the first and second reactor cooling circuits [1, 2]. To substantiate the possibility of operating steam generators with such defects in the area of welded joint No. 111, at least until the next scheduled preventive maintenance, modern approaches to the mechanics of fracture of structural materials with crack-like defects can be applied to predict their behaviour under different loading conditions [2–6]. To perform such calculations, it is very important to have information on the load of the collector to the DN-1200 nozzle welded joint [7–10], including residual stresses associated with the manufacturing or repair technology [11–13].

Experimental determination of residual stresses in thick-walled structures of existing equipment is possible either on the outer surfaces using a standardized method of tensometry [14] or laser speckle interferometry (ESPI–HD method) [15] when drilling a hole, or requires more in-depth studies of a model specimen in the laboratory, for example, by neutron diffraction [16]. It is also advisable to perform finite element modeling of the distribution of residual stresses in the volume of the welded joint [13, 17], which should be

consistent with the results of experimental measurements.

Given the urgency of the problem of damage to welded joint No. 111 for the Ukrainian NPP, it is necessary to determine the reliable distribution of residual technological stresses in the specified joint for the purpose of further calculated justification of its operability with the discontinuity defects identified during operation.

## DESIGN, MATERIALS AND MANUFACTURING TECHNOLOGY OF WELDED JOINT No. 111

Figure 1 shows a layout of the collector welded joint to the DN1200 nozzle of the PGV-1000 steam generators. The DN1200 nozzle of the steam generator and collector are made of 10GN2MFA pearlite steel. The welded joint is made by manual or automatic welding. The root of the weld is made manually by argon arc welding using filler wire Sv08G2S. The height of the root pass is 6–8 mm. The main part of the weld is filled by manual welding using TsU-7 or UONI-13/55 electrodes with a diameter of 4 or 5 mm, and in automatic welding Sv08GSMT and Sv10GN1MA wires with a diameter of 2 mm and FTs-16 or AN-17 flux are used.

To relieve residual stresses associated with either welding during manufacture or repair of individual defects in welded joint No. 111 (Figure 1) detected during operation, a local heat treatment procedure is

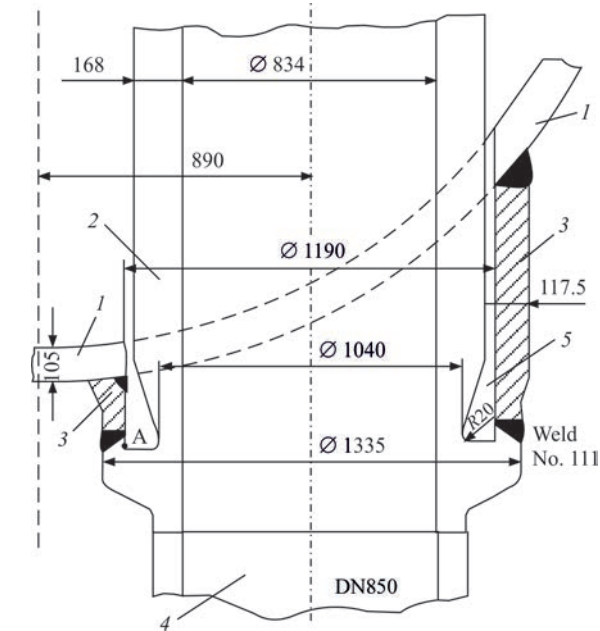


**Figure 1.** Layout of welded joint No. 111: 1 — steam generator case; 2 — collector; 3 — DN1200 nozzle; 4 — DN850 pipeline; 5 — pocket; A — discontinuity defect

performed using a high tempering mode ( $T_{\max} = 650$  °C) with ring heaters.

**THE AIM**

of this paper is to analyse the effect on the residual stress state of local heating of a rather complex geometry of the welded joint between the collector and the steam generator nozzle, which contains an inner pocket between the collector and the nozzle and is not axisymmetric, i.e., has different lengths of the nozzle along the circumferential coordinate. Local postweld heat treatment of such a joint may lead to the formation of new high residual stresses after partial relieving of the residual welding stresses. Therefore, in order to conduct an in-depth analysis of the problem, this paper considers the formation of residual stresses only after local heat treatment, without taking into account the stresses forming after multipass welding. By the method of mathematical modeling in a general three-dimensional formulation, taking into account

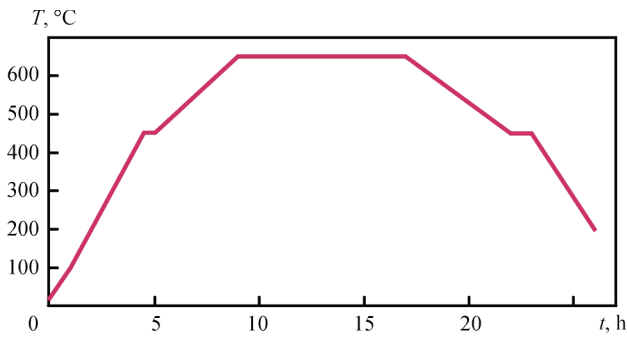


**Figure 3.** Diagram of varying heat treatment temperature in the high tempering mode

the non-axisymmetry of welded joint No. 111, as well as in a two-dimensional axisymmetric formulation, the distribution of residual stresses as a result of local heat treatment alone was calculated.

Two options of postweld local heat treatment are considered, namely, during the manufacturing process and during in-service repair. These options differ in the number of local heating zones. During the manufacture of the steam generator in the factory conditions, welded joint No. 111 has access to heating from the inside of the collector (Figure 2, a). During the repair of welded joint No. 111 at NPP, when the steam generator collector is connected to the DN850 pipeline of the first circuit, there is no possibility of heating from the inside of the collector (Figure 2, b), which can significantly affect the temperature distribution during postweld local heat treatment.

In the area where the heating elements are located (Figure 2), the surface temperature changes over time (from the start of the heat treatment operation) in accordance with the diagram in Figure 3. The rest of the heated surface of the joint is subject to convection heat exchange with the environment with appropriate heat transfer coefficients for the outer surface of the joint, which is specially covered with heat-insulating materials, as well as for the inner surface of the pocket, where convection heat exchange is limited.

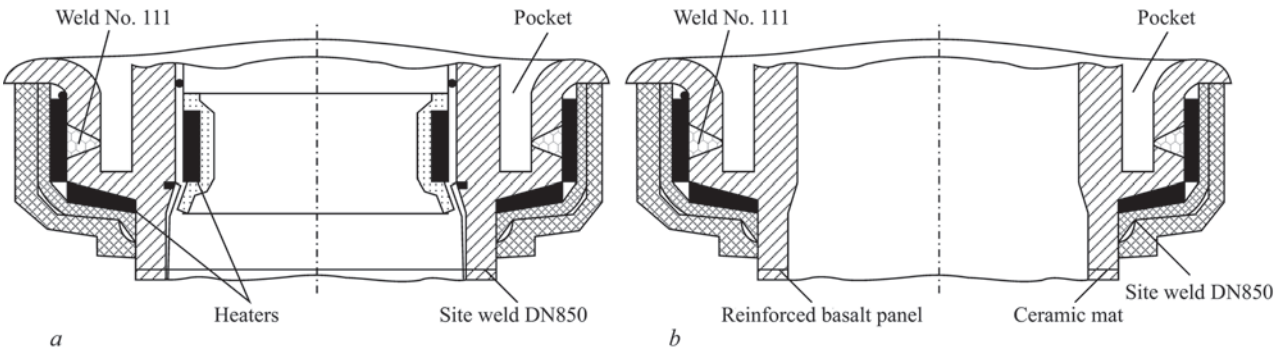


**Figure 2.** Layout of heaters and heat-insulating materials on welded joint No. 111 during local postweld heat treatment: a — during the manufacture of the steam generator in the factory conditions; b — during the repair of the welded joint at NPP

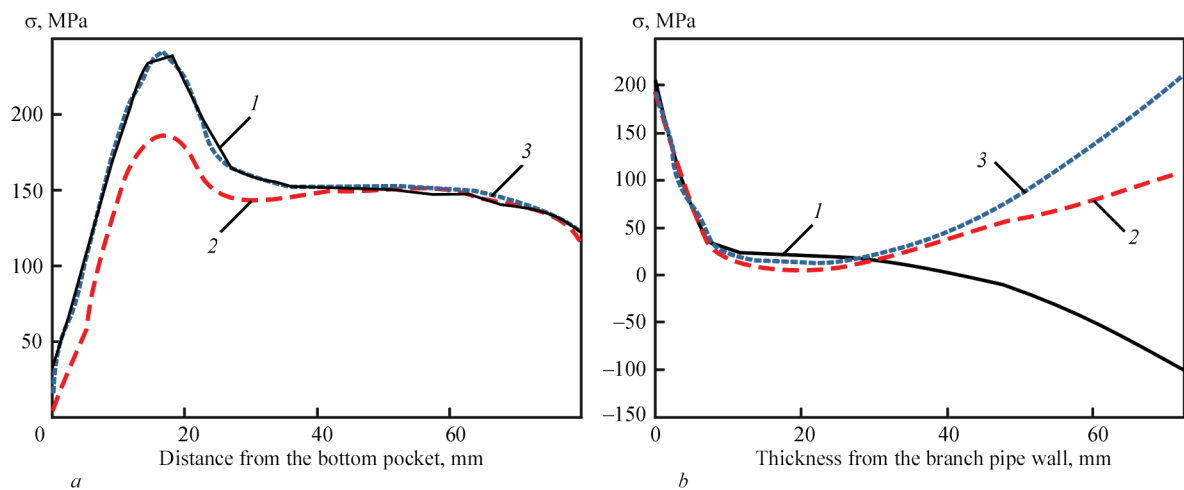


**Figure 4.** Distribution of axial  $\sigma_z$  (1), circumferential  $\sigma_\beta$  (2) and equivalent  $\sigma_1$ – $\sigma_3$  (3) residual stresses on the surface of the pocket on the side of the nozzle (a) and over the thickness of its wall (b), starting from the point with the maximum stress (based on the results of two-dimensional calculations [11])

### EXISTING DATA ON THE DISTRIBUTION OF RESIDUAL STRESSES

The results of numerical modeling of residual stresses in welded joint No. 111 are shown in Figure 4 [11]. It is seen that at the specified heating areas and modes of factory heat treatment, as well as the physical and mechanical properties of the material (10GN2MFA steel), local heating of the joint causes local temperature expansion of the heated area and the development of plastic compression strains in the axial and tangential directions on the inner surface of the pocket on the side of the nozzle. In the areas of inelastic compression, residual tensile stresses occur during further cooling. The distribution of the axial stress component on the surface of the pocket on the nozzle side has a characteristic maximum in the area of the fillet transition at a distance of about 17 mm from the bottom of the pocket (Figure 4, a). In addition to the axial component, high circumferential residual tensile

stresses are formed over the thickness of the nozzle closer to the inner surface (Figure 4, b). The increased stresses formed as a result of heat treatment, taking into account their concentration in the area of defects, may cause crack initiation.

### DEVELOPMENT OF A MATHEMATICAL MODEL FOR DETERMINING RESIDUAL STRESSES AFTER LOCAL HEAT TREATMENT OF WELDED JOINT No. 111

To calculate the residual stresses, a general 3D finite element model of the welded joint of the collector to the DN1200 nozzle was developed, taking into account the variable length of the nozzle along the circumferential coordinate ( $H \approx 240$ – $920$  mm) (Figure 5), as well as a simplified axisymmetric 2D model (Figure 6) with the length of the nozzle equal to the minimum value in the actual structure.

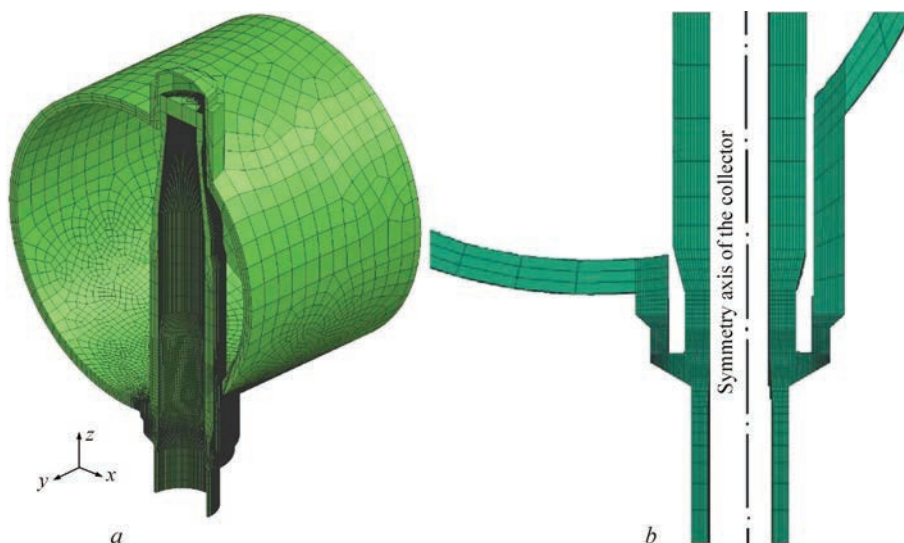


**Figure 5.** Finite element 3D model of welded joint No. 111 of the PGV-1000 steam generator: a — general appearance; b — cross section



**Figure 6.** Finite element axisymmetric 2D model of welded joint No. 111

The ring heating sources (heaters), which provide local heat treatment of the welded joint, were simulated by the corresponding heat flow through the heating surface according to the specified programme, as indicated for the high tempering mode (Figure 3). Schemes of 3D and 2D models of the welded joint and a finite element mesh are shown in Figures 5 and 6, respectively. The temperature dependences of the thermophysical and mechanical properties of 10GN2MFA steel are given in Table 1.

The kinetics of temperature distributions during local heat treatment was determined by solving the nonstationary heat conduction equation:

$$\begin{aligned} c\rho \frac{\partial T}{\partial t} = \frac{\partial}{\partial x} \left( \lambda \frac{\partial T}{\partial x} \right) + \frac{\partial}{\partial y} \left( \lambda \frac{\partial T}{\partial y} \right) + \\ + \frac{\partial}{\partial z} \left( \lambda \frac{\partial T}{\partial z} \right), \end{aligned} \quad (1)$$

where  $T$  is the temperature, °C;  $c$  is the specific heat capacity, J/kg·°C;  $\rho$  is the density, kg/m<sup>3</sup>;  $\lambda$  is the thermal conductivity, W/(m·°C).

The peculiarity of the model of the heating source for local heat treatment is the heat dissipation (heat flux) through the contact surfaces of the heaters. In the absence of data on the heat output of the heaters, the time-varying heat flux on the contact surface of the heaters into the material of the joint was set through the boundary conditions of contact heat exchange with the heater at a temperature  $T_H(t)$ , as specified for the high tempering mode (Figure 3):

$$q_H(t) = \lambda \frac{\partial T}{\partial n} = -h_H(T_H(t) - T), \quad (2)$$

where  $h_H$  is the heat transfer coefficient to the joint material from the heaters, the value of  $h_H = 150 \text{ W/(m}^2\cdot\text{°C)}$  was chosen from the condition of ensuring the heating rate of the welded joint metal of 45–100 °C/h in accordance with the high tempering mode.

Boundary conditions on the surfaces of the models of the joint, taking into account convection heat exchange with the environment, were set in the form:

$$q = \lambda \frac{\partial T}{\partial n} = -h(T_0 - T), \quad (3)$$

where  $q$  is the heat flux on the surface of the joint elements;  $T_0$  is the ambient temperature;  $h$  is the heat transfer coefficient from the surface during convection heat exchange with the environment. Typically,  $T_0 = 20 \text{ °C}$ ,  $h = 15 \text{ W/(m}^2\cdot\text{°C)}$  from the surface under conditions of natural convection in the air; when installing heat-insulating materials,  $h = 2 \text{ W/(m}^2\cdot\text{°C)}$  can be accepted.

The model of thermoviscoplastic deformation of the welded joint material assumes that the total strain tensor is the sum of elastic, plastic and creep strains:

**Table 1.** Mechanical and thermophysical properties of 10GN2MFA steel depending on temperature [5]

Temperature $T$ , °C	Young's modulus $E \cdot 10^{-5}$ , MPa	Yield strength $\sigma_y(T)$ , MPa	Thermal conduc- tivity $\lambda$ , J/(cm <sup>3</sup> ·°C)	Volumetric heat capacity $c\gamma$ , J/(cm <sup>3</sup> ·°C)	Poisson's ratio $\mu$	Coefficient of linear expansion $\alpha$ , 1/°C
100	2.01	488	0.375	3.88	0.25	1.14
200	1.96	466	0.370	3.98	0.25	1.18
300	1.90	443	0.360	4.21	0.25	1.22
350	1.87	415	0.355	4.44	0.25	1.25
400	1.85	380	0.350	4.76	0.25	1.30
500	1.78	355	0.337	5.10	0.25	1.34
600	1.70	300	0.320	5.80	0.25	1.39
700	1.60	200	0.305	7.35	0.25	1.42
800	1.50	60	0.285	8.10	0.25	1.47
900	1.35	40	0.280	5.60	0.25	1.52
1000	1.15	20	0.275	5.00	0.25	1.65
1100	1.00	20	0.270	4.90	0.25	1.70
1200	1.00	20	0.267	4.90	0.25	1.62



$$\varepsilon_{ij} = \varepsilon_{ij}^e + \varepsilon_{ij}^p + \varepsilon_{ij}^c \quad (i, j = x, y, z). \quad (4)$$

The components of the stress and elastic strain tensors are related by Hooke's law:

$$\varepsilon_{ij}^e = \frac{\sigma_{ij} - \delta_{ij}\sigma}{2G} + \delta_{ij}(K\sigma + \varphi), \quad i, j = x, y, z, \quad (5)$$

where  $\delta_{ij}$  is a unit tensor ( $\delta_{ij} = 0$  if  $i \neq j$ ,  $\delta_{ij} = 1$  if  $i = j$ );

$\sigma = \frac{1}{3}(\sigma_{xx} + \sigma_{yy} + \sigma_{zz})$ ;  $G = \frac{E}{2(1+\nu)}$  is the shear

modulus;  $K = \frac{1-2\nu}{E}$  is the volume compressibility;

$E$  is the Young's modulus;  $\nu$  is the Poisson's ratio;  $\varphi$  is the function of free relative elongations caused by temperature changes:

$$\varphi = \alpha(T - T_0), \quad (6)$$

$\alpha$  is the coefficient of relative temperature elongation of the material.

Plastic strains are related to the stress state by the equation of the theory of plastic non-isothermal flow and the associated Mises flow condition:

$$d\varepsilon_{ij}^p = d\lambda(\sigma_{ij} - \delta_{ij}\sigma), \quad i, j = x, y, z, \quad (7)$$

where  $d\varepsilon_{ij}^p$  is the increment of the tensor  $\varepsilon_{ij}^p$ , which at a set time  $t$  is determined by the history of deformation, stresses  $\sigma_{ij}$  and temperature  $T$ ;  $d\lambda$  is the scalar function determined by the flow conditions:

$$\begin{aligned} d\lambda &= 0, \text{ if } f = \sigma_i^2 - \sigma_T^2(T) < 0 \text{ or } f = 0 \text{ at } df < 0; \\ d\lambda &> 0, \text{ if } f = 0 \text{ and } df > 0; \\ \text{the state } f > 0 &\text{ is unacceptable,} \end{aligned}$$

$\sigma_i$  is the stress intensity;  $\sigma_T(T)$  is the yield strength of the material at temperature  $T$ .

For the creep strains  $d\varepsilon_{ij}^c$  the coupling equation in the form of [5] is used:

$$d\varepsilon_{ij}^c = \Omega(\sigma_i, T)(\sigma_{ij} - \delta_{ij}\sigma)dt, \quad (8)$$

where  $\Omega(\sigma_i, T)$  is the scalar creep function of the material at temperature  $T$  and stress level determined by the stress intensity  $\sigma_i$ .

For this problem, when during heat treatment it is most important to take into account the creep strains  $d\varepsilon_{ij}^c$  since the process of stress relieving significantly depends on them, it is rational to choose the function  $\Omega(\sigma_i, T)$  on the basis of experiments on deformation at elevated temperatures of specimens of this material.

Accordingly, the creep function in general form as a function of material temperature, starting from a

temperature of 550 °C and above, can be approximated by the typical dependence:

$$\Omega(\sigma_i, T) = A \cdot \sigma_i^n \cdot \exp\left(\frac{G}{T + 273}\right), \quad (9)$$

where  $A$ ,  $G$  are constants related to material properties.

The presented model of creep at elevated temperatures is quite general and allows tracing deformation processes during heat treatment not only during holding, but also during heating and cooling at temperatures, for example, 550 °C and above. This model can be effective in simulating residual stress relaxation processes during local heat treatment of welded structures or in the case of furnace heat treatment with a short holding time, when uniform heating to a set holding temperature is not ensured over the volume of the welded structure or joint.

The coefficients of the creep function for the base material of the welded joint (10GN2MFA steel) were determined in [5] based on the processing of existing experimental data [18] in accordance with the degree of relaxation of residual tensile stresses  $\sigma_{xx}$  during the holding period  $t = 2$  h of heat treatment after welding plates made of 10GN2MFA steel, depending on the tempering temperature  $T = 550\text{--}700$  °C. Table 2 shows the results of calculating the constants of the creep function (8) using experimental data.

In the mathematical modeling of the stress-strain state in the considered joint, even in the absence of residual stresses before local heat treatment, it is advisable to take into account creep processes, since during local heat treatment, temporary temperature stresses are formed, under the influence of which, during long-term exposure at elevated temperatures, significant plastic strains can be formed by the creep mechanism.

The peculiarities of the mathematical model of non-isothermal deformation of the material during local thermal tempering of welded joint No. 111 at a maximum temperature of up to 650 °C are boundary conditions corresponding to the free fixation of the model; absence of structural phase changes and corresponding volume effects; stress relieving due to the processes of instantaneous ductility and temperature creep of the material, which is taken into account by the creep function  $\Omega(\sigma_i, T)$ . Since the residual welding stresses are not taken into account, the formation and development of new residual stresses during lo-

**Table 2.** Parameters of creep function  $\Omega(\sigma_i, T)$  for 10GN2MFA steel in the temperature range  $550 < T < 700$  °C [5]

$n$	$A$ , $\text{MPa}^{-(n+1)} \cdot \text{h}^{-1}$	$G$ , °C
5	$8.46 \cdot 10^{17}$	-66394

cal heat treatment occurs due to a significant heating nonuniformity over the volume of the welded joint. During long-term holding (9 h), thermal stresses are partially relieved due to material creep and plastic strains are formed, which can also affect the level of residual stresses.

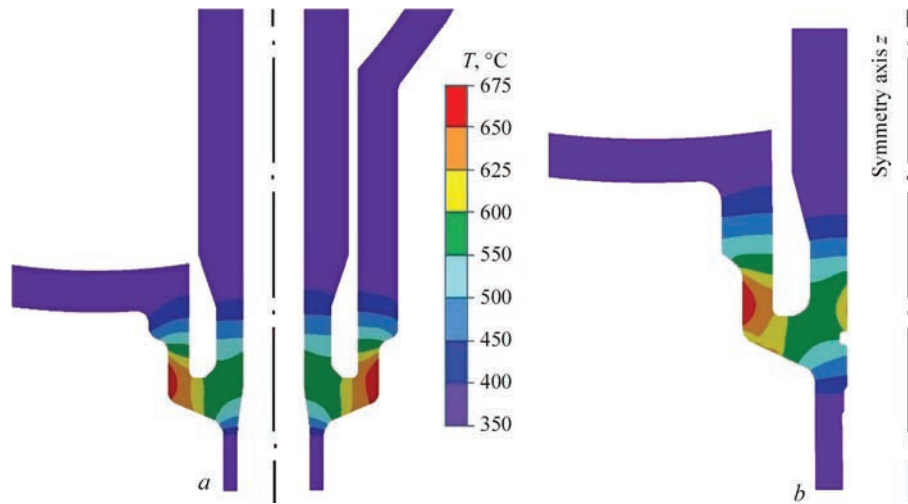
RESULTS OF THE SIMULATION

Figure 7 shows the distributions of maximum temperatures at holding during local postweld heat treatment in the high tempering mode at  $T = 650\text{ }^{\circ}\text{C}$ , obtained for 2D and 3D models of welded joint No. 111. Due to the complex geometry of the joint, heating using locally arranged heaters does not ensure uniform temperature distribution in the welded joint zone during heat treatment (Figure 7).

From the point of view of ensuring the integrity of welded joint No. 111 under the stress corrosion failure mechanism, the distributions of circumferential and axial residual stresses on the inner surface of

the joint is of particular importance. As a result, significantly nonuniform heating causes the formation of high residual stresses (Figure 8). On the inner surface, the circumferential stresses  $\sigma_{\beta\beta}$  reach the level of 350 MPa, and on the outer surface — up to 300 MPa (Figure 8, *a*). The axial tensile stresses  $\sigma_{zz}$  on the inner surface reach 400 MPa, and the compressive stresses on the outer surface reach up to 300 MPa (Figure 8, *b*). The radial stresses in the zone of deposited metal are negligible, but a zone of rather high tensile stresses of up to 100 MPa is formed on the inner surface in the zone of radial transition of the pocket (Figure 8, *c*).

Figure 9 shows the calculated distributions of residual stresses over the thickness of welded joint No. 111 after local heat treatment (factory mode) without simulation of welding process ( $T = 650\text{ }^{\circ}\text{C}$ , holding time  $t = 8\text{ h}$ ), obtained using 2D and 3D models in comparison with existing data [11]. The results for the axial component  $\sigma_{zz}$  are quite similar in nature of distribution (Figure 9, *a*). Thus, according to the



**Figure 7.** Distributions of maximum temperatures at holding during local heat treatment in the high tempering mode at  $T = 650\text{ }^{\circ}\text{C}$ : *a* — 3D model, repair heat treatment mode; *b* — 2D model, factory heat treatment mode

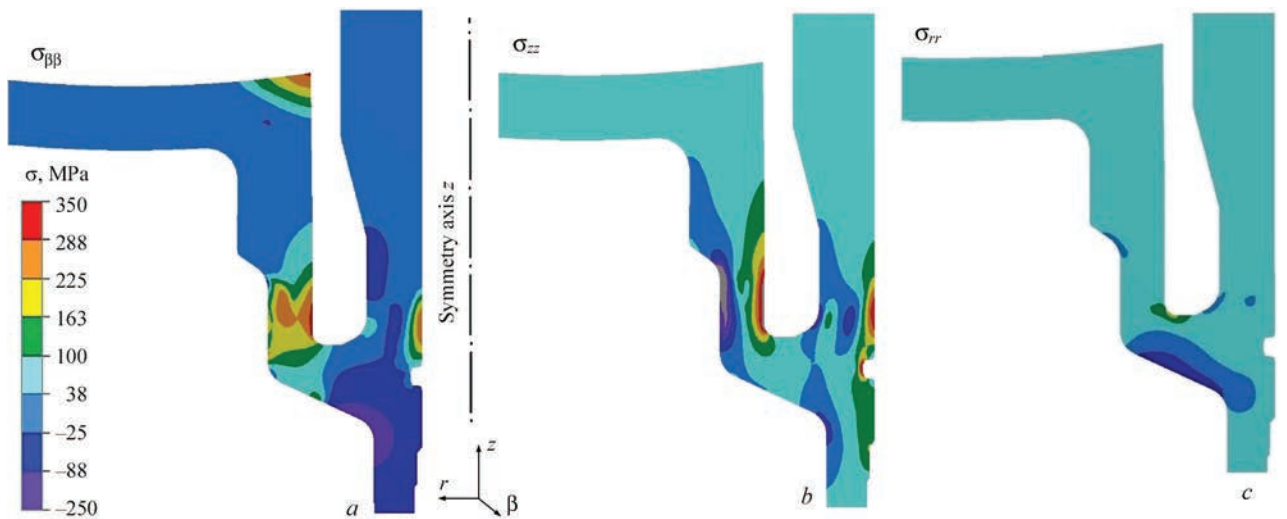


**Figure 8.** 2D model. Residual stresses in welded joint No. 111 after local heat treatment (factory heat treatment mode) without welding simulation ( $T = 650\text{ }^{\circ}\text{C}$ , holding time  $t = 8\text{ h}$ ), MPa: *a* — circumferential  $\sigma_{\beta\beta}$ ; *b* — axial  $\sigma_{zz}$ ; *c* — radial  $\sigma_{rr}$

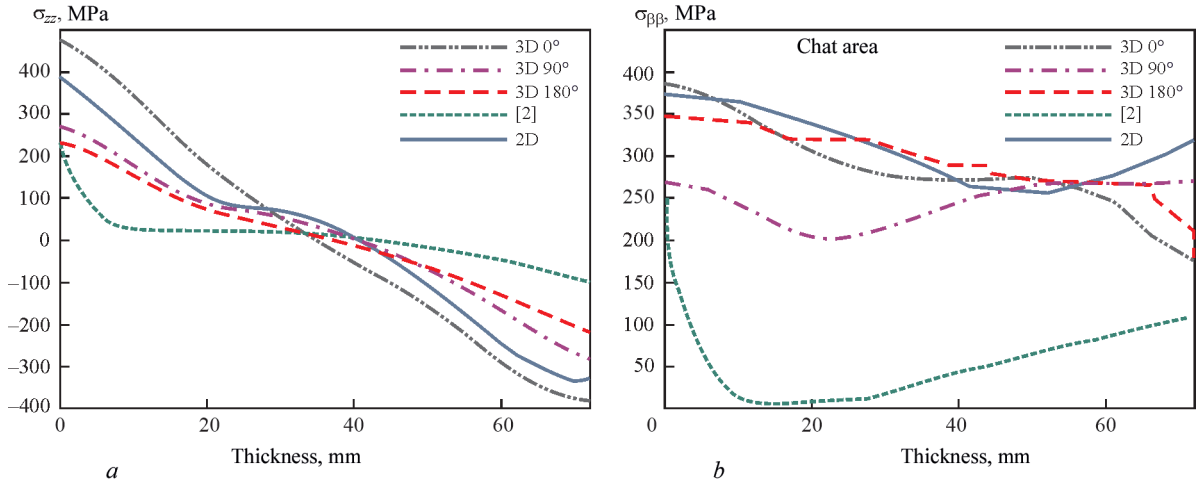


**Figure 9.** Distribution of residual stresses over the thickness of welded joint No. 111 after local heat treatment (factory mode) ( $T = 650^\circ\text{C}$ , holding time  $t = 8\text{ h}$ ):  $a$  — axial component  $\sigma_{zz}$ ;  $b$  — circumferential component  $\sigma_{\beta\beta}$  (for the 3D model, the angular coordinate is calculated from the smallest nozzle length  $\varphi = 0^\circ$ , respectively, the largest nozzle length corresponds to  $\varphi = 180^\circ$ )

obtained data, on the outer surface of the joint, the axial residual stresses are compressive, and on the inner surface they are tensile, but differ significantly in absolute value. According to the existing data, tensile stresses reach 230 MPa, according to the results of the 2D model — almost 400 MPa, and the 3D model gives different values depending on the angular coordinates  $\varphi$ , namely, from 220 MPa in the area with a high nozzle height ( $\varphi = 180^\circ$ ) to 480 MPa in the area with a low nozzle height ( $\varphi = 0^\circ$ ).

As for the circumferential component  $\sigma_{\beta\beta}$  (Figure 9,  $b$ ), according to the existing data, the residual stresses on the inner surface of the joint are tensile of up to 250 MPa, and then drop sharply to almost zero values. The residual stresses obtained using 2D and 3D models are tensile over the entire thickness of the joint, but on the inner surface, according to the 2D model, they are up to 370 MPa, and according to the 3D model, they are from 270 MPa ( $\varphi = 180^\circ$ ) to 380 MPa ( $\varphi = 0^\circ$ ).

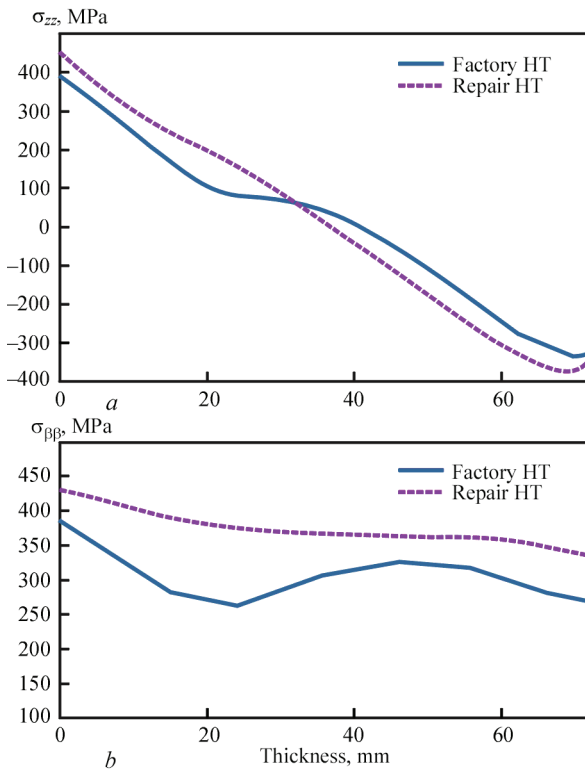


**Figure 10.** Distribution of residual stresses over the thickness of welded joint No. 111 after local factory or repair heat treatment ( $T = 650^\circ\text{C}$ , holding time  $t = 8\text{ h}$ ):  $a$  — axial component  $\sigma_{zz}$ ;  $b$  — circumferential component  $\sigma_{\beta\beta}$

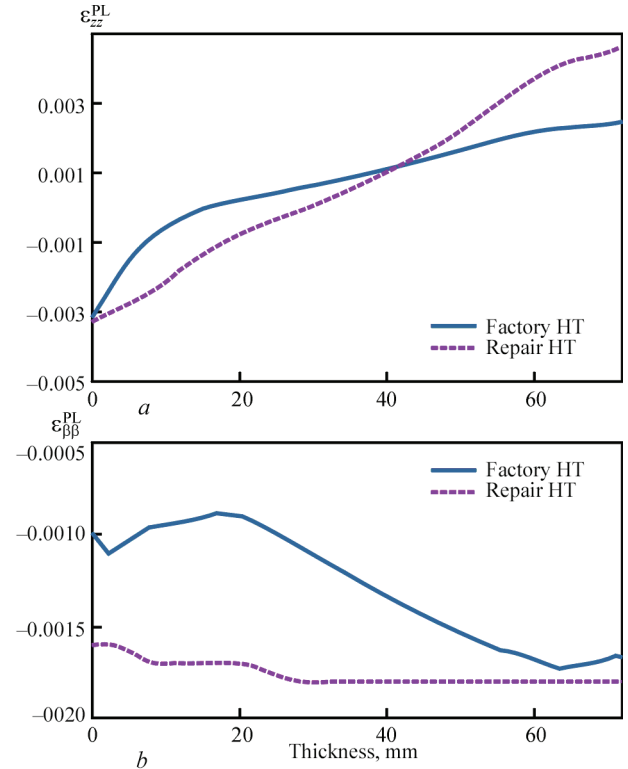


**Figure 11.** Distribution of plastic strains over the thickness of welded joint No. 111 after local factory or repair heat treatment ( $T = 650^\circ\text{C}$ , holding time  $t = 8\text{ h}$ ):  $a$  — axial component  $\epsilon_{zz}^p$ ;  $b$  — circumferential component  $\epsilon_{\beta\beta}^p$

The presented results showed that, firstly, according to existing data [11], the residual tensile stresses on the inner surface of welded joint No. 111 after local heat treatment are significantly lower than those obtained in this study using 2D and 3D models. Secondly, the use of an axisymmetric 2D model with a short nozzle length provides rather conservative results compared to the 3D model.

Another problem investigated in this work is the difference in residual stresses after local heat treatment in the factory mode, when there is access to the inner surface of the collector, where an additional heater can be placed (Figure 2, *a*), and in the repair mode, when the heaters are located only on the outside of the joint (Figure 2, *b*).

Figures 10 and 11 show the calculated results obtained using the 2D model for the distributions of residual stresses and plastic strains over the thickness of welded joint No. 111 after local heat treatment according to the factory and repair heat treatment modes without simulation of welding process ( $T = 650\text{ }^{\circ}\text{C}$ , holding time  $t = 8\text{ h}$ ). It can be clearly seen that the repair local heat treatment is associated with a higher level of residual stresses on the inner surface of the joint, by about 10–15 %.

Assuming that the residual welding stresses relieving to a large extent at holding during heat treatment, new residual stresses are formed during cooling. This is especially true in the metal close to the inner surface, where rather high (up to 350–450 MPa) circumferential and axial residual tensile stresses are formed.

The presented results on the study of the effectiveness of the technology of local heat treatment of welded joint No. 111 showed that an unsuccessful choice or limited possibilities for the arrangement of heaters during local heat treatment can lead to negative consequences, namely, the formation of new residual tensile stresses in dangerous areas of the welded joint.

The obtained prediction results apply to all joints No. 111 of both hot and cold collectors, since individual deviations related to the size of the development, the number of passes, the parameters of the welding and heat treatment mode within the considered technological process do not significantly affect the final results. The low efficiency of the considered technology of postweld heat treatment and, possibly, even its negative impact on the integrity of welded joint No. 111 indicate the need in optimizing the technology of local heat treatment using mathematical modeling methods.

## CONCLUSIONS

The results of mathematical modeling of the residual stresses of the welded joint of the collector to the

DN1200 nozzle of the PGV-1000 steam generators (welded joint No. 111) as a result of local heat treatment under the high tempering mode without taking into account the residual stresses after welding showed that:

1. The inner surface of the joint in the area of welded joint No. 111 has rather high residual tensile stresses (up to 350–450 MPa) both in the circumferential and axial directions due to significant nonuniform heating over the thickness and creep processes during high temperature holding.

2. The axisymmetric 2D finite element model of the joint with a small nozzle DN1200 provides sufficient conservatism of the results compared to the 3D model, significantly reduces the requirements for computational resources and can be used to calculate residual stresses after multipass welding and subsequent local heat treatment.

3. Local heat treatment during the repair of welded joint No. 111 at NPP is associated with a higher level of residual tensile stresses on the inner surface of the joint (by about 10–15 %) than during the manufacture of the steam generator in the factory conditions, when it is possible to access the inner surface of the collector, where an additional heater can be placed.

4. An inappropriate choice or limited possibilities for the arrangement of heaters during local heat treatment of welded joint No. 111 can lead to negative consequences, namely the formation of new high residual tensile stresses in dangerous areas of the welded joint.

## REFERENCES

1. Voyevodin, V.N., Ozhigov, L.S., Mitrofanov, A.S. et al. (2014) Identification of defects in the welded joint metal of the case of steam generator to the collector on the WVER-1000. *Voprosy Atomnoi Nauki i Tekhniki*, 4(92), 82–87 [in Russian].
2. Dub, A.V., Durynin, V.A., Razygraev, A.N. et al. (2014) Development of ultrasonic testing procedures and determination of performance of the assembly of the joint of header to steam generator PGV-1000M. *Tekh. Diagnost. i Nerazrush. Kontrol*, 4, 36–51 [in Russian].
3. Kharchenko, V.V., Chirkov, A.Yu., Kobel'skii, S.V., Kravchenko, V.I. (2017) Improving the computational analysis of stress-strain state and fracture resistance of welded joints between coolant headers and PGV-1000M steam generator vessel of nuclear power station. *Strength of Materials*, 49, 349–360. DOI: <https://doi.org/10.1007/s11223-017-9875-3>
4. Makhnenko, V.I., Markashova, L.I., Makhnenko, O.V. et al. (2012) Growth of corrosion cracks in structural steel 10GN2MFA. *The Paton Welding J.*, 8, 2–5.
5. Makhnenko, V.I. (2006) *Safe service life of welded joints and assemblies of modern structures*. Kyiv, Naukova Dumka [in Russian].
6. Stepanov, G.V., Shirokov, A.V. (2014) Assessment of the kinetics of crack propagation in the header-steam generator connector welded joint No. 111 by plasticity resource. *Strength of Materials*, 46, 375–382. DOI: <https://doi.org/10.1007/s11223-014-9559-1>



7. Stepanov, G.V., Kharchenko, V.V., Babutskii, A.I. et al. (2003) Stress-strain state evaluation of a welded joint of hot collector to nozzle of NPP steam generator PGV-1000. *Strength of Materials*, **35**, 536–544. DOI: <https://doi.org/10.1023/B:STOM.0000004543.31528.98>
8. Kharchenko, V.V., Stepanov, G.V., Kravchenko, V.I. et al. (2009) Redistribution of stresses in the header-PGV-1000 steam generator connector weldment under loading after thermal treatment. *Strength of Materials*, **41**, 251–256. DOI: <https://doi.org/10.1007/s11223-009-9130-7>
9. Khodakovskii, A.A., Chirkov, A.Yu., Kharchenko, V.V. (2013) Calculation analysis of the stress-strain state of the collector-to-nozzle weld in the steam generator under seismic loading. *Strength of Materials*, **45**, 482–488. DOI: <https://doi.org/10.1007/s11223-013-9483-9>
10. Banko, S. (2012) Stressed state of the collector-case connection unit of the PGV-1000M steam generator with a cavity. *Visnyk Ternopilskoho NTU*, 67(3), 56–63 [in Ukrainian].
11. Stepanov, G.V., Kharchenko, V.V., Babutskii, A.I. (2006) Stress-strain state of the header-steam generator connector weldment induced by local thermal treatment. *Strength of Materials*, **38**, 595–600. DOI: <https://doi.org/10.1007/s11223-006-0081-y>
12. Muzhychenko, O.F., Makhnenko, O.V. (2019) Mathematical modeling of residual stresses in the collector to nozzle Du1200 welding unit of steam generators PGV-1000. In: *Proc. of the Intern. Conf. on Innovative Technologies and Engineering in Welding and Related Processes PolyWeld 2019, May 23–24, 2019, Kyiv*, 82–83.
13. Makhnenko, O.V., Milenin, O.S., Muzhychenko, O.F. et al. (2023) Mathematical modeling of residual stress relaxation during performance of postweld heat treatment. *The Paton Welding J.*, **6**, 32–40. DOI: <https://doi.org/10.37434/tpwj2023.06.05>
14. (2015) ASTM E837-13a. *Standard Test Method for Determining Residual Stresses by the Hole-Drilling Strain-Gage Method*. ASTM International.
15. Lobanov, L., Pivtorak, V., Savitsky, V., Tkachuk, G. (2014) Technology and equipment for determination of residual stresses in welded structures based on the application of electron speckle-interferometry. *Mat. Sci. Forum*, **768–769**, 166–173. DOI: <https://doi.org/10.4028/www.scientific.net/MSF.768-769.166/>
16. Rogante, M. (2020) Inside welds: Advanced characterization of residual stresses by neutron diffraction. *The Paton Welding J.*, **11**, 18–24. DOI: <https://doi.org/10.37434/tpwj2020.11.04>
17. Senchenkov, I.K., Chervinko, O.P., Banyas, M.V. (2013) Modeling of thermomechanical process in growing viscoplastic bodies with accounting of microstructural transformation: *Encyclopedia of Thermal Stresses*. Springer Ref., **6**, 3147–3157.
18. Hrivnak, I. (1984) *Weldability of steels*. Ed. by E.L. Makarov. Moscow, Mashinostroenie [in Russian].

## ORCID

O.V. Makhnenko: 0000-0002-8583-0163,  
O.F. Muzhychenko: 0000-0002-4870-3659

## CONFLICT OF INTEREST

The Authors declare no conflict of interest

## CORRESPONDING AUTHOR

O.V. Makhnenko  
E.O. Paton Electric Welding Institute of the NASU  
11 Kazymyr Malevych Str., 03150, Kyiv, Ukraine.  
E-mail: [makhnenko@paton.kiev.ua](mailto:makhnenko@paton.kiev.ua)

## SUGGESTED CITATION

O.V. Makhnenko, O.F. Muzhychenko, I.I. Prudkiy, N.R. Basistyuk (2025) Residual stresses in the joint of the collector to the DN1200 nozzle of the PGV-1000 steam generator due to local heat treatment. *The Paton Welding J.*, **11**, 19–27. DOI: <https://doi.org/10.37434/tpwj2025.11.03>

## JOURNAL HOME PAGE

<https://patonpublishinghouse.com/eng/journals/tpwj>

Received: 27.02.2025

Received in revised form: 18.05.2025

Accepted: 21.11.2025



## NEW BOOK

**Akhonin S.V., Berezos V.O., Yerokhin O.H. Producing high-strength titanium alloys by the method of electron beam melting.** — Kyiv: E.O. Paton Electric Welding Institute of the NAS of Ukraine, 2025. — 128 p. (in Ukrainian).

The monograph deals with the features of producing ingots of complex titanium alloys by the method of electron beam melting. The mechanisms and regularities of alloying element behaviour when producing ingots of complex high-strength titanium alloys by the method of cold-hearth electron beam melting were studied. Taking into account the established dependencies, the optimal technological modes of producing complex titanium alloys by the method of electron beam melting were proposed for titanium alloy VT9, which provide a high level of qualitative and technical-economic parameters. The characteristics of chemical composition, state of the surface, macro- and microstructure of the ingots of commercial and new local complex titanium alloys are presented. The question of deformation processing of the produced alloys is considered and mechanical characteristics of semi-finished products from ingots produced by the method of electron beam melting are given.

The book is designed for scientific and engineering workers, as well as for students of metallurgical specialities. 178 Ref., 23 Tables, 91 Figures.

Orders send to E-mail: [patonpublishinghouse@gmail.com](mailto:patonpublishinghouse@gmail.com)